JOURNAL OF MATERIALS SCIENCE 20 (1985) 501–507

The post-yield behaviour of low-density polyethylenes

Part 1 *Strain hardening*

P. J. MILLS*, J. N. HAY, R. N. HAYWARD†
Department of Chemistry, The University of Birmingham, Birmingham, UK

The post-yield behaviour of linear low-density and high-pressure polymerized low-density polyethylenes have been compared in tension and compression. Rubber elasticity theory has been used to describe the strain-hardening region of the stress–strain curves in terms of extension of amorphous regions and entanglement associated with crystalline regions. The resulting strain-hardening functions were used to predict the geometry of the neck profiles produced while deforming in tension. No relationship between strain hardening and environmental stress-crack resistance was found in that the two types of polyethylenes exhibited very different dependences.

1. Introduction

Yield deformation, post-yield and ultimate fracture behaviour of polyethylenes are complex functions of their undeformed morphologies, and the corresponding changes which develop on drawing. The initial morphology, the degree of crystallinity, and mechanical properties are intimately linked to the molecular parameters of branch type and chain length and branch distributions [1]. A study of low-density polyethylenes differing with respect to these parameters should accordingly yield information on the interplay of morphology and mechanical properties.

The investigation of stress–strain behaviour in uniaxial tension is complicated by localized deformation resulting in the formation of a "neck" [2]. This results in a complex sample geometry which makes the measurement of the true stress–strain relationship in the post-yield region indeterminate [3]. However, necked material re-drawn parallel to the original draw direction deforms uniformly and so eliminates any geometric problems.

Similar studies can also be made under plane strain compression [4] where true stress can be measured directly up to true strains of 0.6. Above this value, however, deviations from plane strain conditions become increasingly important.

The present paper considers the success of such procedures in assessing the strain-hardening properties of different low-density polyethylenes – linear copolymers (LLDPE) and high-pressure low-density polyethylenes (LDPE). Marked variations between the two were observed which not only usefully separated them, but also demonstrated the applicability of the experimental procedure and analyses of strain hardening in terms of network deformation. Although it was appreciated that the two types of polyethylene have differences in both distribution and type of branch which produce initial variations in crystalline morphology, no attempt was made to compare fractions of similar degree of branching, this being the subject of subsequent papers. Instead bulk polymers were matched for melt-index, crystallinity and degree of branching, and observable variations in the strain-hardening behaviour and characteristic of the commercial polymers.

2. Experimental details

Sclair and Dowex LLDPE samples were kindly provided by DuPont (Canada) Chemicals Ltd and

*Present address: Department of Materials Science and Engineering, Cornell University, Bard Hall, Ithaca, New York 14853, USA.
†Present address: Farmgate House, 1A Gaddum Road, Bowdon, Cheshire, UK.

0022–2461/85 $03.00 + .12

TABLE I Polyethylene characteristics

Serial no.	Manufacturer	Grade no.	Density ($g\,cm^{-3}$)	Melt index ($dg\,min^{-1}$)
S1	Dupont Chem. Co Ltd	11B	0.922	0.70
S2	Dupont Chem. Co Ltd	8105	0.921	2.35
S3	Dupont Chem. Co Ltd	8107	0.921	4.24
S4	Dupont Chem. Co Ltd	8109	0.923	8.71
D1	Dow Chem. Co Ltd	2045	0.920	1.15
D2	Dow Chem. Co Ltd	2035	0.919	4.11
BX1	B.X. Co Ltd	N80433	0.918	0.07
BX2	B.X. Co Ltd	DFDG4262	0.922	0.84
BX3	B.X. Co Ltd	N81382	0.921	4.31
BX4	B.X. Co Ltd	DFDG0989	0.928	1.91

Dow Chemicals Ltd, respectively. LDPE samples were provided by B.X.L. Ltd. The polymer characteristics are listed in Table I.

1 and 6 mm thick sheets, 20 cm × 20 cm, were moulded at 450 K for 5 min under a pressure of $4\,MN\,m^{-2}$ and quenched directly into iced water. These sheets were used for tensile and plane strain compression tests, respectively.

Plane strain testing was carried out in a manner previously described, using an Instron tensometer, model TT-BM. Polymer Laboratory Ltd's Minimat microscope extensometer [5, 6] was used for tensile tests. Both types of experiment were conducted at 295 K and a relative humidity of 50%.

True tensile stress–strain relationships for the strain-hardening region in tensile deformation were obtained from dumb-bell samples cut parallel to the original draw direction from previously drawn material. The strain was measured by direct observation of the deformation of a gold/palladium alloy square grid pattern evaporated under vacuum through a fine metal gauge (50 to 400 lines per inch) on to the surface of the specimen [5, 6]. Only strains above the initial draw value were used in the subsequent analysis of the stress–strain data.

Stress crack measurements were made under constant strain using a modified Bell-type test. The active solution was 20% vol/vol aqueous Igepal at 323 K. Samples of dimensions 4.5 cm × 1.3 cm × 0.15 cm were slit through the centre, bent into a "U" shape and inserted into an 18 mm diameter test tube. Ten specimens of each sample were used and the time required for half of them to fracture, F_{50}, was taken as a measure of the environmental stress crack resistance.

Density measurements were made with a density column of formamide and *n*-propanol. Melt-index was measured with a Davenport Extrusion Plastimeter according to BS 2782 method 105C.

3. Results and discussion

3.1. Strain hardening

Ductile polymers when deforming continuously and uniformly above the yield point are progressively strain hardened whereby increased deformation requires the application of an increased load. Typical stress–strain curves for compression and tensile tests in the range of strain of interest are shown for both LLDPE and LDPE in Fig. 1.

A model for the strain-hardening behaviour of polymers has been proposed by Haward and Thackray [7]. This sets out to describe stress–strain curves in terms of elastic, viscous (yielding) and strain-hardening elements. The strain-hardening process which was initially the novel element in the model may be related to the well-established rubber elasticity theory [9], of which several different equations have been reported in the literature [10, 11]. Recently, more conventional rubber elasticity equations have been found to give better results as well as being simpler than the Langevin functions originally employed [8]. Such treatments also provide a better route to understanding material behaviour than the several empirical relationships which have also been used to describe strain hardening. The theoretical basis of the various elasticity equations is provided in standard texts of which we used Treloar [9].

Assuming that there is little change in internal energy of the polymer on deformation and that the polymer chains assume a Gaussian distribution, then in uniaxial tension:

$$\sigma_T = G(\lambda^2 - 1/\lambda), \quad (1)$$

and in plane strain compression:

$$\sigma_T = G(\lambda^2 - 1/\lambda^2), \quad (2)$$

in which

$$G = \rho RT/M_e, \quad (3)$$

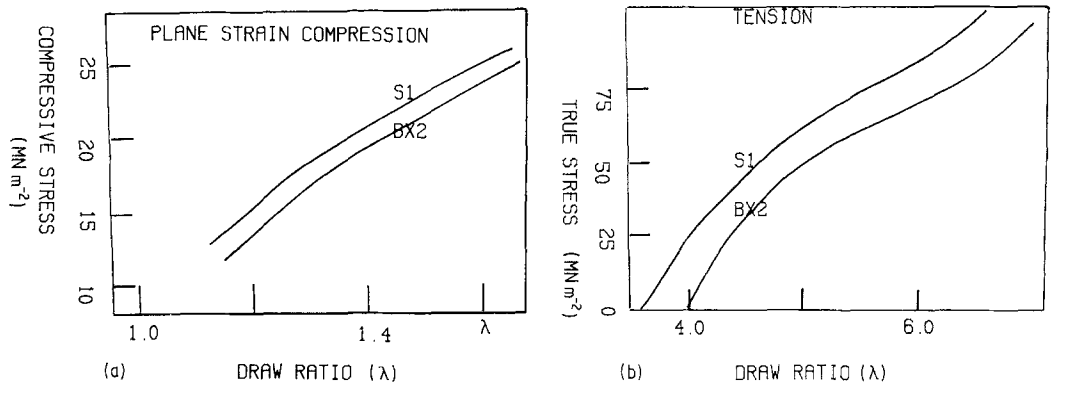

Figure 1 Typical stress–draw ratio curves for LDPE, i.e. BX2, and LLDPE; i.e. S1. (a) Plane strain compression, (b) tension.

σ_T is the true stress, λ the draw ratio, ρ the density, R the gas constant, T the temperature and M_e the entanglement molecular weight, i.e. the molecular weight of the segments between two adjacent permanent entanglements.

In the Mooney–Rivelin theory of rubber elasticity, the assumption of Gaussian distribution of molecular chain segments is not invoked. Instead the equation is derived from considerations of the symmetry of deformation. The resulting expression for tension is:

$$\sigma_T = 2K_1(\lambda^2 - 1/\lambda) + 2K_{11}(\lambda - 1/\lambda^2), \quad (4)$$

and for plane strain compression:

$$\sigma_T = 2(K_1 + K_{11})(\lambda^2 - 1/\lambda^2). \quad (5)$$

Since $K_1/K_{11} = 10$, the two sets of Equations 1 and 4, and 2 and 5 are almost identical [8].

Plots of tensile stress, σ_T, against $(\lambda^2 - 1/\lambda)$ are shown in Fig. 2, and a linear relationship was observed only above the initial yield stress used in producing the drawn specimen. However, the compression stress gave a linear dependence with $(\lambda^2 - 1/\lambda^2)$, see Fig. 3 from the initial readings.

Figs. 2 and 3 give convincing evidence for the applicability of the Mooney–Rivelin treatment to both plane-strain compression and tension. From the two component model, the intercept at $\lambda = 1$ is the yield stress of the polymer. The intercepts are in reasonable agreement with that measured separately in tension i.e. $10\,MN\,m^{-2}$ for $0.920\,g\,cm^{-3}$ low-density polyethylene samples [12]. The slope of the plots from the various polyethylene samples is a measure of the elastic modulus, G. These are listed in Table II and plotted as a function of melt flow index in Fig. 3. It can be seen that for both LDPE and LLDPE there is a decrease in the value of G with increasing melt flow index. However, a greater dependence was observed with LLDPE than LDPE. From Equation 3 the decrease in G is

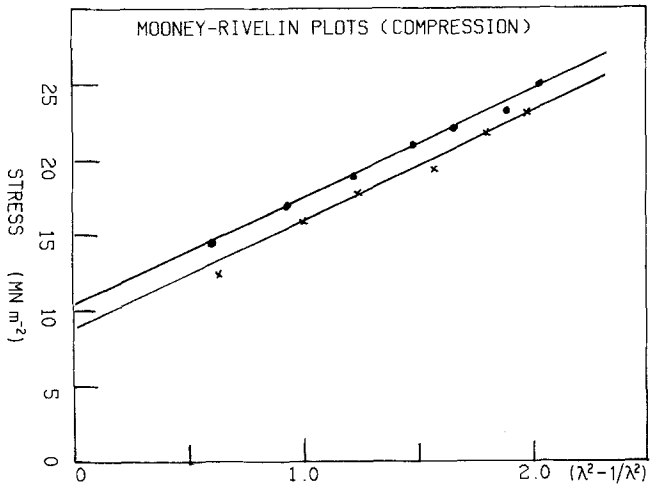

Figure 2 Mooney–Rivelin plots of plane strain compression data; •, S1; ×, BX2.

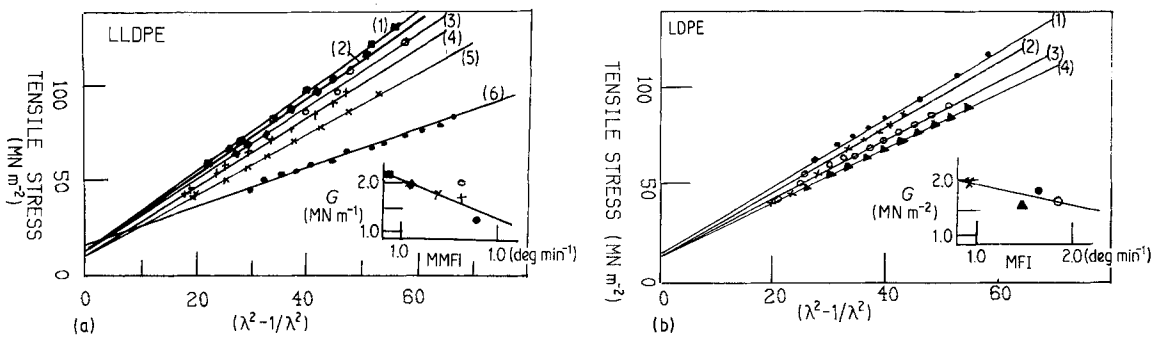

Figure 3 Mooney–Rivelin plots of tensile stress–strain data and the variation of G with melt index. (a) LLDPE: (1) S1; (2) D1; (3) S3; (4) D2; (5) S2; (6) S4. (b) LDPE: (1) BX1; (2) BX2; (3) BX3; (4) BX4.

associated with an increase in molecular weight between entanglements, see Table II. Graessley and Edwards [13] have derived a value obtained from the plateau modulus in the visco-elastic response of concentrated polyethylene solutions to be equal to 1750 g mol^{-1}. Considering experimental differences between the two methods of measurement, this value is in reasonable agreement with those listed in Table II.

Melting studies have confirmed that for low-density polyethylene, deformation in the post-yield region is accompanied by little or no change in the crystallite size distribution, suggesting that the deformation is mainly associated with extensions of amorphous regions alone [1, 12]. The crystalline regions will, however, clearly have a substantial effect on the amorphous network, acting as anchor points for tie molecules and possibly as entanglements, for the network.

Crystallization studies on branched polyethylenes have shown that branches greater than 2 carbon atoms long are excluded from the crystalline regions and so the lamellar sizes and their distribution are controlled by the segment molecular weight between branch points. Assuming that the branches are placed randomly and that there is a random distribution of segments placed in the lamellae, then the molecular weight of the segments of chains in the amorphous regions, i.e. between adjacent crystalline segments is given by:

$$M_A = \xi(1 - X_c)/X_c, \qquad (6)$$

in which ξ is the number average lamellar degree of polymerization, and X_c the volume fraction of crystalline material.

Values of X_c and ξ were determined by differential scanning calorimetry and gel permeation chromatography of nitric acid etched material, respectively [1]. The calculated values of M_A are listed in Table II. These values are in substantial agreement with those of M_e.

While the nature of the network which is being deformed remains uncertain and more studies on amorphous polymers and crystalline polymers of different lamella size distributions are required, it is apparent that deformation of the amorphous matrix in which lamellae are embedded, could account for the strain-hardening characteristics.

TABLE II Strain-hardening characteristics

	Serial no.	Melt index (dg min^{-1})	G (MN m^{-2})	M_e (g mol^{-1})	M_a (g mol^{-1})
(a) LLDPE	S1	0.70	2.14	980	1100
	S2	2.35	1.74	1200	1050
	S3	4.24	2.00	1050	1070
	S4	8.71	0.98	2140	1030
	D1	1.15	1.92	1090	1120
	D2	4.11	1.68	1250	1130
(b) LDPE	BX1	0.07	2.20	950	910
	BX2	0.84	1.54	1360	840
	BX3	4.31	1.66	1260	860
	BX4	1.91	1.88	1120	880

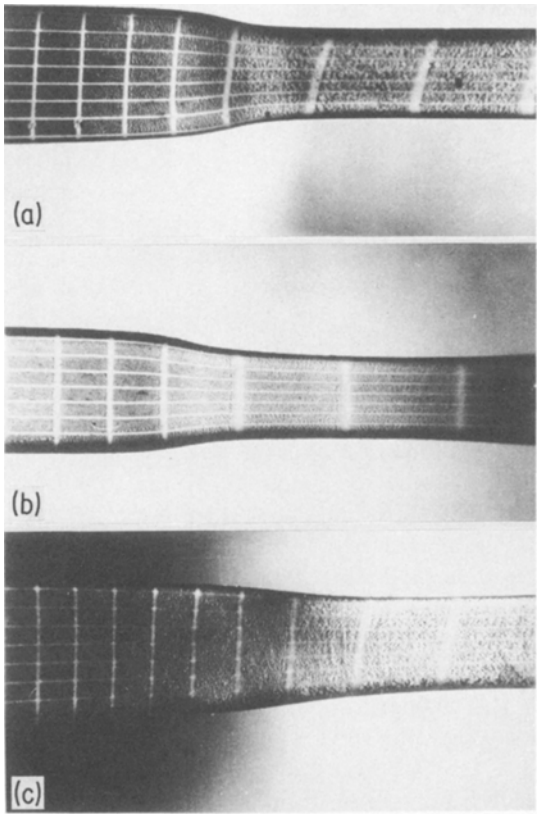

Figure 4 The variation of neck profile with the Mooney–Rivelin modulus G. (Undeformed grid equals 50 lines per inch.) LLDPE: (a) S1, $G = 2.1\,MN\,m^{-2}$; (b) S2, $G = 1.7\,MN\,m^{-2}$; (c) S4, $G = 1.0\,MN\,m^{-2}$.

3.2. The application of strain hardening to necking

The profiles of the necks observed in the various grades of LLDPE can be seen in Fig. 4. They were consistent with the anticipated trend of a more diffuse neck being associated with more pronounced strain hardening.

The simple model of neck propagation, as suggested initially by Ward and Coates [14] was used to analyse the necks of the LLDPE samples, see Fig. 5. AB is the isotropic boundary which moved with a constant velocity, V_p, as the neck propagates through the specimen. The draw ratio changes progressively through the neck profile and is dependent on the position, x, along the draw direction, i.e. $\lambda(x)$. Each volume element experiences in turn a changing axial stress $\sigma(x)$, and strain rate $\dot{\epsilon}(x)$. The latter during the progress of the neck moves through a maximum value, since initially

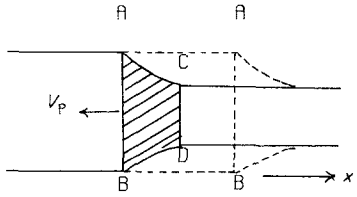

Figure 5 Geometric model of the neck profile, after [14].

and finally it is assumed that

$$\dot{\epsilon}(x) = 0. \tag{7}$$

Owing to the changing geometry, the true axial strain rate is a function of position, x, i.e.

$$\dot{\epsilon}(x) = V_p[d\lambda(x)/d(x)]. \tag{8}$$

The total change in stress arises both from the changes in draw ratio and also the strain rate, and so

$$d\sigma_T = (d\sigma_T/d\lambda)_{\dot{\epsilon}} d\lambda + (d\sigma_T/d\dot{\epsilon})_\lambda d\dot{\epsilon} \tag{9}$$

for which

$$d\dot{\epsilon} = [d\sigma_T - (d\sigma_T/d\lambda)_{\dot{\epsilon}} d\lambda]/(d\sigma_T/d\dot{\epsilon}_T)_\lambda. \tag{10}$$

From the strain-rate sensitivity of the yield stress [1] and by the use of the strain-hardening functions, values of $d\dot{\epsilon}$ were calculated at each value of x for a neck propagating with a constant well-defined profile. By using the deformation characteristics of the neck profile as defined by the changing dimensions of the metal grids evaporated on the surface of the samples as they progressed through the neck profile, the experimental strain rates were determined as a function of draw ratio. These are compared with the calculated values in Fig. 6. Considering the limitations of the model and experimental technique, good agreement was observed between the calculated and observed dependences. This not only suggests that the correct form of the strain hardening function has been derived but also indicates its importance in neck formation.

3.3. Strain hardening and environmental stress cracking

When polyethylene is immersed in certain liquids, fracture may occur in a brittle mode under low stress. This is known as environmental stress cracking, and has been extensively studied [15]. The resistance of polyethylene grades to stress cracking has been attributed to their ability to strain harden. Accordingly, this was examined further.

Haward and Owen [16] have considered the

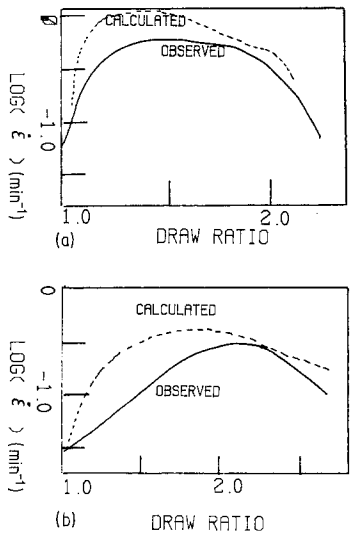

Figure 6 Calculated and observed strain rate changes through the neck profile: (a) S2, (b) S1.

energy required to propagate the stress crack to contain three main components:

1. that required to produce the plastic deformation associated with the crack propagating;

2. strain hardening of the fibrils in the craze leading to an increased volume of deformed material;

3. the energy associated with the production of the new surfaces.

In order to consider effect 2 in determining the environmental stress crack resistance for both LLDPE and LDPE, a comparison was made between the degree of strain hardening exhibited in tensile deformation and the measured valued values of F_{50}.

Fig. 7 shows the variations of the measured stress crack resistances to be strongly dependent on melt flow index. Greater differences existed, however, between the LLDPE and LDPE; indeed the former

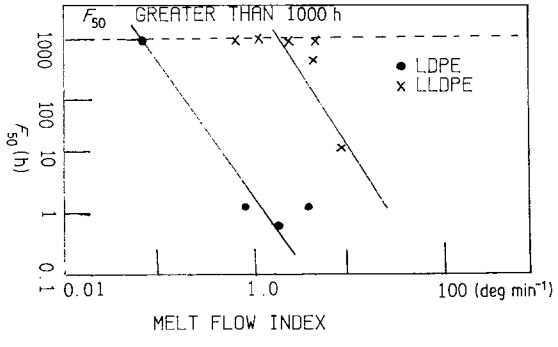

Figure 7 Melt index dependence of the environmental stress crack resistance for LLDPE and LDPE.

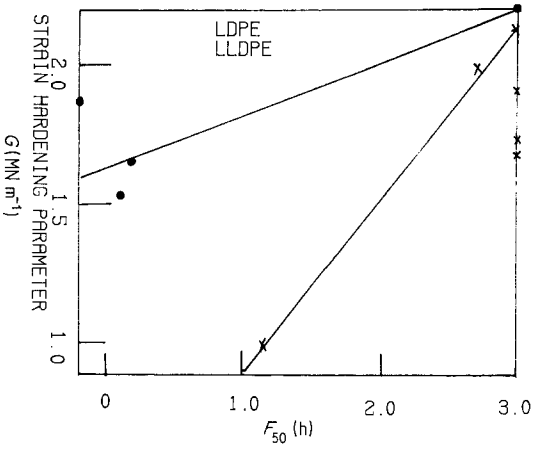

Figure 8 The dependence of environmental stress crack resistance on elastic modulus, G, for LLDPE and LDPE.

polymers have F_{50} values which are in excess of the useful characteristics of the test. Although from Fig. 8 there is evidence for some correlation between stress crack resistance and the strain-hardening parameters of Equation 1, the different resistances for the two types of polyethylenes are not reflected in the strain-hardening parameters and so clearly the ability of a given polyethylene to strain harden is not, as has been claimed previously, the dominant parameter in determining its environmental stress crack resistance.

4. Conclusions

Both in tension and plane strain compression, strain hardening can be correlated with the deformation of an entangled network and rubber elasticity theory can be successfully applied. The elastic moduli, G, and similarly K_1, can be correlated with an entanglement molecular weight, Whilst this value is in reasonable agreement with that obtained from solution, it can also be related to the average molecular weight of the amorphous segments between adjacent lamellae. This suggests strongly that only the amorphous region is deformed in the drawing process, and the hard crystalline regions act as entanglements for the amorphous network.

Viscous flow and strain-dependent components determine the observed neck profiles. Strain hardening alone cannot explain the superior stress crack resistance of LLDPE compared to LDPE.

Acknowledgements

We are indebted to the S.E.R.C. and B.P. Chemicals Ltd for the joint sponsorship of a Case Award for PJM during the course of this work.

References

1. P. J. MILLS, PhD thesis, University of Birmingham (1982).
2. R. N. HAWARD (ed), "Physics of Glassy Polymers" (Applied Science, London 1973), Ch. 6, pp. 348–53.
3. C. G'SELL and J. J. JONES, *J. Mater. Sci.* **14** (1979) 583.
4. J. G. WILLIAMS, *Trans. J. Plastics Inst.* (1967) 505.
5. N. WALKER, J. N. HAY and R. N. HAWARD, *J. Mater. Sci.* **14** (1979) 1085.
6. *Idem, ibid.* **16** (1981), 817.
7. R. N. HAWARD and G. THRACKRAY, *Proc. Roy. Soc.* **A302** (1968) 453.
8. A. CROSS and R. N. HAWARD, *Polymer* **19** (1978) 677.
9. L. R. G. TRELOAR, "The Physics of Rubber Elasticity" (Oxford University Press, London 1975).
10. S. C. BAUWEN, *J. Mater. Sci.* **13** (1978), 1443.
11. R. N. HAWARD, *Coll. and Polymer. Sci.* **258** (1980), 42.
12. A. TRAINOR, R. N. HAWARD and J. N. HAY, *J. Polymer. Sci. Polymer Phys. Ed.* **15** (1977) 1077.
13. W. W. GRAESSLEY and S. F. EDWARDS, *Polymer* **22** (1981) 1329.
14. I. M. WARD and P. D. COATES, *J. Mater. Sci.* **15** (1980) 2897.
15. J. B. DeCOSTE, F. S. MALM and T. WALLDER, *Ind. Eng. Chem.* **43** (1951) 117.
16. R. N. HAWARD and D. R. J. OWEN, *Proc. Roy. Soc.* **A352** (1977) 505.

Received 10 October 1983
and accepted 10 April 1984